# On the prediction of dynamic thermal comfort under uniform environments

Marika Vellei, Jérôme Le Dréau

WINDSOR 2020

# On the prediction of dynamic thermal comfort under uniform environments

**Marika Vellei[1] and Jérôme Le Dréau[1]**

[1] LaSIE (UMR CNRS 7356) - La Rochelle University, La Rochelle, France
corresponding author: marika.vellei@univ-lr.fr

**Abstract:** To help researchers to evaluate uniform but not stationary (thus transient) thermal conditions, we describe, show the performances and provide a new simple tool, which can be used to predict the whole-body dynamic thermal sensation and thermal comfort. The tool comprises a thermo-physiological model able to predict the body core and mean skin temperatures under uniform and transient environmental conditions and a dynamic thermal perception model, which uses the simulated temperatures to predict thermal sensation and thermal comfort. The selected thermo-physiological model is an updated version of the classical Gagge's two-node model. For predicting the thermal sensation vote, we use an updated version of Fiala's Dynamic Thermal Sensation (DTS) model. Finally, for modelling the last step of thermal perception, i.e. thermal comfort, we derive a new dynamic version of the well-known Fanger's Predicted Percentage of Dissatisfied (PPD) index. We show that our novel models have better performances than the original ones. Furthermore, their simplicity and low computational cost are important advantages over more complex and computationally expensive multi-segment and multi-node thermo-physiological models.

**Keywords:** dynamic thermal comfort, Gagge's two-node model, Fiala's Dynamic Thermal Sensation model, Fanger's PPD model

## 1. Introduction

The physical interaction between an occupant and a dynamic indoor environment can be modelled by mathematical models of human thermoregulation, which predict detailed body core and skin temperatures [1]. The predicted temperatures can then be used as inputs for thermal perception models, which are developed from regression analysis of experimental thermal sensation and/or thermal comfort votes and simulated or monitored physiological parameters [2].

Even though several multi-segment and multi-node thermo-physiological models have been developed in recent years (e.g. Tanabe [3], Fiala [4,5], the Berkeley Comfort Model [6] and ThermoSEM [7]), yet they have not been largely applied for the prediction of thermal sensation and thermal comfort in the built environment. These models simulate body core and skin temperatures for different regions of the human body under asymmetric environmental conditions. Their complexity (and the computational burden associated with their implementation) is of little utility in most building energy simulations, which only provide average environmental conditions for the simulated thermal zones. Moreover, the high level of insulation of new buildings leads to little asymmetry and rather homogenous temperature distributions.

In practice, building modellers continue to stick to the traditional Fanger's PMV/PPD model, even for the evaluation of dynamic conditions characterized by rapid changes in either environmental or personal variables [8–15]. However, Fanger's model is derived from a steady-state heat balance equation and steady-state laboratory experiments [16] and is, therefore, only suited to predict thermal comfort under steady-state or slowly changing

indoor conditions (temperature gradients less than 2 °C/h) [2]. Furthermore, the model is not able to predict thermal comfort under dynamic levels of activity.

To help researchers to break away from the bad habit of using the PMV/PPD model when evaluating uniform but not stationary (thus transient) conditions, we describe, test and provide a new simple tool for the prediction of the whole-body dynamic thermal sensation and thermal comfort. The novel tool comprises two main elements:

- a thermo-physiological model able to simulate the body core and mean skin temperatures under uniform conditions,
- a dynamic thermal perception model which uses the simulated body core and mean skin temperatures to predict both thermal sensation and thermal comfort.

The selected thermo-physiological model is an updated version of the classical Gagge's two-node model, also known as Pierce's two-node model [17]. For predicting the dynamic thermal sensation, we opt for an updated version of Fiala's Dynamic Thermal Sensation (DTS) model [18]. Finally, for predicting the dynamic thermal comfort we derive a new model, which is able to calculate the Dynamic Percentage of Dissatisfied (DPD) from the dynamic thermal sensation, thus mimicking the structure of the classical Fanger's PPD index. The original Gagge's and Fiala's models are reviewed in Section 2.1, 2.2 and 2.3. The derivation of the updated Gagge's two-node model is illustrated in Section 4.1. The development of the two parts, i.e. thermal sensation and thermal comfort, of the novel dynamic thermal perception model is illustrated in Section 4.2 and 4.3, respectively.

## 2. Literature

### 2.1. Gagge's two-node model

In Gagge's two-node model, the human body (i.e. the passive/controlled system of human thermoregulation) is simulated as two concentric thermal compartments: a core cylinder (simulating muscle, subcutaneous tissue and bone) surrounded by a thin skin outer layer. The model simulates the heat transfers between the two compartments and between the outer layer and the environment and the temperature within each compartment is assumed to be uniform. The active/controlling system (which simulates the regulatory responses of shivering, vasoconstriction, vasodilatation and sweating) is based on a simple linear, temperature-based control theory of human thermoregulation.

The model was originally developed in 1971 [17,19] and has undergone many iterations and refinements, so that several versions are now available. The version of the model that was used in this work is mainly based on the BASIC and C++ code provided by Fountain and Huizenga [20–22] and has been re-coded in Python and validated against simulated data provided by Haslam [23], which uses a similar version of the model.

Several researchers have tested the performances of Gagge's model against experimental data [21,23,24] and have shown that:

- the model's predictions are very accurate in neutral conditions, reasonable for warm and hot conditions and less accurate in the colder environments (for air temperatures less than 5°C),
- the model is not able to accurately predict conditions of moderate to high exercise intensity (approximately 3.5 met to 8 met), especially during complex fluctuations, characterized by short work and rest cycles.

For additional information on the performances of the model the reader is referred to the works of Haslam [23], Doherty & Arens [21] and Smith [24]. In this paper, a small validation of the model is carried out in Section 5.1.

### 2.2. Fiala's DTS model

The literature offers three main models for predicting the thermal sensation in steady-state and transient conditions from physiological states (inputs parameters are shown in parenthesis):

- Fiala model ($\Delta T_{core}$, $\Delta T_{sk,mean}$, $\frac{\partial T_{sk,mean}}{\partial t}$) [18],
- Zhang model ($\Delta T_{sk,mean}$, $\Delta T_{sk,local}$, $\frac{\partial T_{sk,local}}{\partial t}$) [25–27],
- Takada model ($\Delta T_{sk,mean}$, $\frac{\partial T_{sk,mean}}{\partial t}$) [28].

where $\Delta T_{core}$, $\Delta T_{sk,mean}$, $\Delta T_{sk,local}$ are the differences between the body core, mean skin and local skin temperatures in the actual conditions and their values for thermo-neutral conditions (neutral points); $\frac{\partial T_{sk,mean}}{\partial t}$ and $\frac{\partial T_{sk,local}}{\partial t}$ are the rates of change (first derivatives with respect to time) of the mean and local skin temperatures, respectively. Between the three models we opted for Fiala's DTS model, which has been shown to perform better than the other two for both steady-state and transient exposures [2] and which does not require local skin temperatures as inputs.

Fiala's DTS model was developed from regression analysis of selected experiments including 220 exposures to air temperatures ranging between 13°C and 48°C and activity levels between 1 met and 10 met [18]. The model is able to predict the whole-body thermal sensation on the seven-point ASHRAE scale and is composed of three main parts:

- a first part, as a function of $\Delta T_{sk,mean}$, to model the response of sedentary subjects under steady-state environmental conditions,
- a second part, as a function of $\Delta T_{core}$ weighted by $\Delta T_{sk,mean}$, accounting for effects associated with exercise and warm body core temperatures,
- a third part, as a function of both positive and negative $\frac{\partial T_{sk,mean}}{\partial t}$, dealing with the dynamic components of thermal sensation observed in transient thermal conditions.

Fiala refers to the first and second parts as *the static comfort model*, while the third part represents *the dynamic component* of the human thermal sensation. The complete model has the following form:

$$\boldsymbol{DTS = 3 \cdot tanh\left[a \cdot \Delta T_{sk,mean} + g + \left(0.114 \cdot \frac{\partial T_{sk,mean}}{\partial t}^{(-)} + 0.137 \cdot e^{-0.681t} \cdot \frac{\partial T_{sk,mean}}{\partial t}^{(+)}_{max}\right) \cdot \frac{1}{(1+g)}\right]} \quad (1)$$

where $a$ is 0.301°C$^{-1}$ and 1.078°C$^{-1}$ for $\Delta T_{sk,mean} < 0$ and $\Delta T_{sk,mean} > 0$, respectively. $\frac{\partial T_{sk,mean}}{\partial t}^{(-)}$ is equal to 0 for $\frac{\partial T_{sk,mean}}{\partial t} > 0$ and $g$ is calculated from:

$$\boldsymbol{g = 7.94 \cdot e^{\left(\frac{-0.902}{\Delta T_{core}+0.4} + \frac{7.612}{\Delta T_{sk,mean}-4}\right)}} \quad (2)$$

where $g = 0$ for $\Delta T_{core} \leq -0.4\ K$ or $\Delta T_{sk,mean} \geq 4\ K$. Thus, the effect of $g$ on thermal sensation vanishes for either cold core temperatures or too warm skin temperatures.

The term $0.114 \cdot \frac{\partial T_{sk,mean}}{\partial t}^{(-)}$ of the dynamic component accounts for overshoots (i.e. abrupt decreases) of thermal sensation caused by transient cooling of the skin. The term $0.137 \cdot e^{-0.681t} \cdot \frac{\partial T_{sk,mean}}{\partial t}^{(+)}_{max}$ represents the time-weighted maximum positive rate of

change of the skin temperature and accounts for abrupt increases of thermal sensation caused by transient warming of the skin. This dynamic term is based on Fiala's assumption that, during skin warming, the thermal sensation is governed by the most intense rate of change of skin temperature, weighted by a function of the time elapsed since its occurrence. Cooling and warming overshoot responses appear under both cold and warm skin conditions and have been first observed by Gagge during temperature step-change variations [29]. During exercising conditions, the thermal sensation is less sensitive to transient changes in skin temperatures, therefore the dynamic component is weighted by $\frac{1}{(1+\mathrm{g})}$, where g is the term responsible for changes in thermal sensation due to exercise.

### 2.3. Fiala's active system model

Fiala's empirical control equations for sweating, shivering, and cutaneous vasomotion (i.e. constriction and dilatation) are derived from statistical analysis of 27 different experiments covering a range of air temperatures between 5°C and 50°C, and exercise intensities between 0.8 met and 10 met [4]. In Fiala's empirical control model, for conditions of internal hot stress, the sweating and vasodilatation responses are described using the warm temperature error signal from the body core $\Delta T_{core}^{(+)}$. While, for conditions characterized by not significant changes in the body core temperature, sweating and vasodilatation are governed by the warm skin temperature error signal $\Delta T_{sk,mean}^{(+)}$. The cold skin temperature error signal $\Delta T_{sk,mean}^{(-)}$ is the governing variable for the responses against cold, i.e. vasoconstriction and shivering. The effect of the cold body core temperature error signal $\Delta T_{core}^{(-)}$ on vasoconstriction is negligible, while it is more substantial for shivering. It is important to highlight that cold skin temperature error signals $\Delta T_{sk,mean}^{(-)}$ have an inhibiting effect on sweating and warm body core temperature error signals $\Delta T_{core}^{(+)}$ have an inhibitory effect on shivering. Furthermore, sweating and shivering can be respectively inhibited and stimulated by negative rates of change of the mean skin temperature $\frac{\partial \mathrm{T_{sk,mean}}^{(-)}}{\partial \mathrm{t}}$. When sweating is elicited due to $\Delta T_{core}^{(+)}$ (e.g. when working in a cold environment) shivering is set to zero.

Fiala's control equation for the cutaneous vasodilatation in W/°C is given by:

$$\boldsymbol{Dl} = \mathbf{16}\cdot\left[\boldsymbol{tanh}\left(\mathbf{1.92}\cdot\boldsymbol{\Delta T_{sk,mean}^{(+)}} - \mathbf{2.53}\right)+\mathbf{1}\right]\cdot\boldsymbol{\Delta T_{sk,mean}^{(+)}} + \mathbf{30}\cdot\left[\boldsymbol{tanh}\left(\mathbf{3.51}\cdot\boldsymbol{\Delta T_{core}^{(+)}} - \mathbf{1.48}\right)+\mathbf{1}\right]\cdot\boldsymbol{\Delta T_{core}^{(+)}} \quad (3)$$

Fiala's control equation for the sweating rate in g/min is given by:

$$\boldsymbol{Sw} = \left[\mathbf{0.65}\cdot\boldsymbol{tanh}\left(\mathbf{0.82}\cdot\boldsymbol{\Delta T_{sk,mean}^{(+,-)}} - \mathbf{0.47}\right)+\mathbf{1.15}\right]\cdot\boldsymbol{\Delta T_{sk,mean}^{(+,-)}} + \left[\mathbf{5.6}\cdot\boldsymbol{tanh}\left(\mathbf{3.14}\cdot\boldsymbol{\Delta T_{core}^{(+)}} - \mathbf{1.83}\right)+\mathbf{6.41}\right]\cdot\boldsymbol{\Delta T_{core}^{(+)}} \quad (4)$$

Fiala's control equation for the cutaneous vasoconstriction, dimensionless, is given by:

$$\boldsymbol{Cs} = \mathbf{35}\cdot\left[\boldsymbol{tanh}\left(\mathbf{0.29}\cdot\boldsymbol{\Delta T_{sk,mean}^{(-)}} + \mathbf{1.11}\right)-\mathbf{1}\right]\cdot\boldsymbol{\Delta T_{sk,mean}^{(-)}} - \mathbf{7.7}\cdot\boldsymbol{\Delta T_{core}^{(-)}} + \mathbf{3}\cdot\boldsymbol{\Delta T_{sk,mean}^{(-)}}\cdot\frac{\boldsymbol{\partial T_{sk,mean}}^{(-)}}{\boldsymbol{\partial t}} \quad (5)$$

Fiala's control equation for the shivering response in W is given by:

$$\boldsymbol{Sh} = \mathbf{10}\cdot\left[\boldsymbol{tanh}\left(\mathbf{0.51}\cdot\boldsymbol{\Delta T_{sk,mean}^{(-)}} + \mathbf{4.19}\right)-\mathbf{1}\right]\cdot\boldsymbol{\Delta T_{sk,mean}^{(-)}} - \mathbf{27.5}\cdot\boldsymbol{\Delta T_{core}^{(-,+)}} - \mathbf{28.2} + \mathbf{1.9}\cdot\boldsymbol{\Delta T_{sk,mean}^{(-)}}\cdot\frac{\boldsymbol{\partial T_{sk,mean}}^{(-)}}{\boldsymbol{\partial t}} \quad (6)$$

## 3. Methods

### 3.1. Used datasets

Dataset 0 was assembled to validate the body core and skin temperatures predicted by the updated Gagge's two-node model and does not include any thermal sensation and/or thermal comfort vote, which are instead part of the other datasets described below. It includes data coming from 5 different experiments carried out by different research teams [30–33]. In the first experiment (Condition 0-1) 3 subjects were exposed to warm step-change exposures from 28.5°C to 37.5°C and back to 28.5°C [34]. In the second experiment (Condition 0-2) 3 subjects were exposed to cold step-change exposures from 29°C to 22°C and back to 29°C [30]. In the third experiment (Condition 0-3) 3 subjects were exposed to an air temperature of 12°C for 90 minutes followed by a sudden change to 28°C [31]. In the fourth experiment (Condition 0-4) 8 subjects were exposed to an air temperature of -10°C for 180 minutes followed by a sudden change to 21.7°C and the metabolic rate was alternately varied between 1.2 and 3 met [32]. Finally, in the fifth experiment (Condition 0-5) 11 subjects were exposed to step-changes in metabolic rates from 2.2 met to 3.5 met and finally to 1 met [33].

Table 1. Details of the experimental conditions included in Dataset 0. The data are used to validate the updated Gagge's two-node model.

| | $T_a$ (°C) | $T_r$ (°C) | **RH** (%) | **V** (m/s) | **clo** | **met** |
|---|---|---|---|---|---|---|
| Condition 0-1 [34] | 28.5-37.5-28.5 | 28.5-37.5-28.5 | 40-33-41 | 0.1 | 0.1 | 1 |
| Condition 0-2 [30] | 29-22-29 | 29-22-29 | 44-39-41 | 0.1 | 0.1 | 1 |
| Condition 0-3 [31] | 12-28 | 12-28 | 45 | 0.2 | 0.1 | 1 |
| Condition 0-4 [32] | -10-21.7 | -10-21.7 | 81-59 | 0.15 | 1.1 | 1.2-3 |
| Condition 0-5 [33] | 30 | 30 | 30 | 0.2 | 0.1 | 2.2-3.5-1 |

Dataset I is used to validate the updated Fiala's DTS model and is made of experimental data collected at Kansas State University [35]. This is one of the very first laboratory experiment investigating cyclical temperature fluctuations. As part of the experiment, 12 students were exposed to 2 different cyclical temperature fluctuations, with each variation having an overall duration of 3 hours (Condition I-1 and I-2 in Figure 4). The study was conducted in summer and was addressing cooling and warming temperature transients in warm conditions. Thermal sensation was monitored every 7.5 minutes.

Table 2. Details of the experimental conditions included in Dataset I. The data are used to validate the updated Fiala's DTS model.

| | $\frac{\partial T_a}{\partial t}_{mean}$ (°C/h) | $T_{a_{mean}}$ (°C) | $T_r$ (°C) | **RH** (%) | **V** (m/s) | **clo** | **met** |
|---|---|---|---|---|---|---|---|
| Condition I-1 [35] | ±10.9 | 27 | 25.6 | 45 | 0.14 | 0.7 | 1 |
| Condition I-2 [35] | ±5 | 27.4 | 25.6 | 45 | 0.14 | 0.7 | 1 |

Dataset II is used to derive the updated Fiala's DTS and Fanger's DPD models and consists of experimental data collected at the University of Sydney [36]. Among the literature of thermal comfort studies investigating cyclical temperature variations, this is the laboratory experiment employing the greatest number of participants exposed to the highest rates of temperature change (up to 30°C/h). As part of the experiment, 56 students were exposed to 6 different cyclical temperature fluctuations (Conditions II-2 to II-7 in Figure 5), with each variation having an overall duration of 2 hours. The study was conducted in summer and was addressing cooling and warming temperature transients in warm conditions. Thermal sensation and thermal acceptability were monitored every 5 minutes.

Table 3. Details of the experimental conditions included in Dataset II. The data are used to derive the updated Fiala's DTS and Fanger's DPD models.

| | $\frac{\partial T_a}{\partial t}_{mean}$ (°C/h) | $\frac{\partial T_r}{\partial t}_{mean}$ (°C/h) | **RH** (%) | **V** (m/s) | **clo** | **met** |
|---|---|---|---|---|---|---|
| Condition II-2 [36] | ±8.8 | ±8.8 | 72 to 86 | up to 0.12 | 0.5 | 1 |
| Condition II-3 [36] | ±13.4 | ±13.4 | 65 to 94 | up to 0.12 | 0.5 | 1 |
| Condition II-4 [36] | ±10.2 | ±10.2 | 70 to 94 | up to 0.12 | 0.5 | 1 |
| Condition II-5 [36] | ±10.3 | ±10.3 | 68 to 82 | up to 0.12 | 0.5 | 1 |
| Condition II-6 [36] | ±10.7 | ±10.7 | 66 to 86 | up to 0.12 | 0.5 | 1 |
| Condition II-7 [36] | ±11.3 | ±11.3 | 64 to 98 | up to 0.12 | 0.5 | 1 |

Dataset III is used to derive the updated Fiala's DTS model and includes experimental data collected at Chongqing University [37,38]. This is one of the most recent laboratory experiment investigating step-change variations, both cool-neutral-cool and warm-neutral-warm transients. As part of the experiment, 12 students were exposed to 3 different cool-neutral-cool variations (Condition III-1: 12-22-12°C, Condition III-2: 15-22-15°C and Condition III-3: 17-22-17°C) in winter and 3 different warm-neutral-warm variations (Condition III-4: 32-25-32°C, Condition III-5: 30-25-30°C and Condition III-6: 28-25-28°C) in summer. Each experiment lasted for 2 hours. Following the step-change transition, thermal sensation and thermal comfort were monitored every 2 minutes.

Table 4. Details of the experimental conditions included in Dataset III. The data are used to derive the updated Fiala's DTS model.

| | $T_a$ (°C) | $T_r$ (°C) | **RH** (%) | **V** (m/s) | **clo** | **met** |
|---|---|---|---|---|---|---|
| Condition III-1 [37] | 12-22-12 | 12-22-12 | 57-44-57 | 0.07-0.01-0.07 | 1.17 | 1 |
| Condition III-2 [37] | 15-22-15 | 15-22-15 | 58-51-58 | 0.03-0-0.03 | 1.17 | 1 |
| Condition III-3 [37] | 17-22-17 | 17-22-17 | 54-49-54 | 0.06-0-0.06 | 1.17 | 1 |
| Condition III-4 [38] | 32-25-32 | 32-25-32 | 59-58-59 | 0.1 | 0.5 | 1 |
| Condition III-5 [38] | 30-25-30 | 30-25-30 | 59-58-59 | 0.1 | 0.5 | 1 |
| Condition III-6 [38] | 28-25-28 | 28-25-28 | 61-61-61 | 0.1 | 0.5 | 1 |

Dataset IV was specifically assembled to validate the updated Fiala's DTS model under dynamic conditions characterized by significant changes in metabolic rates. The dataset includes data coming from 4 different experiments carried out by different research teams [39–42]. In the first experiment (Condition IV-1), 11 subjects alternatively rested for 15 minutes (1 met) and walked slowly (1.5 met). At the same time, they were exposed to cyclical temperature variations at rates of ±18°C/h over a period of 2 hours and their thermal sensation was recorded every 5 minutes [39]. In the second experiment (Condition IV-2), the thermal sensation of 10 subjects was recorded during a work/rest sequence at an air temperature of 10°C. For the first hour of the experiment the subjects exercised on a bicycle (2.6 met) followed by an hour of recovery during which the subjects seated quietly (1 met) [40]. In the third experiment (Condition IV-3), 6 students pedalled on a bicycle (3.6 met) for 90 minutes after resting for 30 minutes (1 met) at an air temperature of 24°C. Their thermal sensation was surveyed each 15 minutes [41]. In the third and fourth experiments (Conditions IV-4 and IV-5), 20 students alternately seated (1 met) and walked at 0.9 m/s (2.0 met) and 1.2 m/s (2.6 met) for 30 minutes at two different air temperatures of 20 and 25°C. Their thermal sensation was recorded each 1 to 5 minutes [42].

Table 5. Details of the experimental conditions included in Dataset IV. The data are used to validate the updated Fiala's DTS model.

| | $\mathbf{T_a}$ (°C) | $\mathbf{T_r}$ (°C) | **RH** (%) | **V** (m/s) | **clo** | **met** |
|---|---|---|---|---|---|---|
| Condition IV-1 [39] | $\frac{\partial T_a}{\partial t}_{mean}$ =±18°C/h | $\frac{\partial T_a}{\partial t}_{mean}$ =±18°C/h | 50 | 0.25 | 0.7 | 1-1.5 |
| Condition IV-2 [40] | 10 | 10 | 52 | 0.1 | 1.2 | 2.6-1 |
| Condition IV-3 [41] | 24 | 24 | 45 | 0.15 | 0.6 | 3.6-1 |
| Condition IV-4 [42] | 20 | 20 | 53 | 0.1 | 0.85 | 1-2-2.6 |
| Condition IV-5 [42] | 25 | 25 | 53 | 0.1 | 0.85 | 1-2-2.6 |

### 3.2. Performance metric

The root-mean-square-error (RMSE) is used to measure the predictive accuracy of the updated models against the original ones.

$$\boldsymbol{RMSE} = \sqrt{\frac{\sum(\boldsymbol{OV} - \boldsymbol{PV})^2}{\boldsymbol{n}}} \quad 7$$

where $OV$ is the observed value, $PV$ is the predicted value and $n$ is the number of data points.

## 4. Updated models

### 4.1. Gagge's two-node model

From the review of Section 2.1 we can conclude that, despite its simple representation of the human body, Gagge's two-node model is mildly accurate to be used for practical applications in the built environment where environmental conditions are usually near the neutrality and activity levels are mostly lower than 3.5 met. However, activities in the built environments can be sometimes characterized by abrupt changes in metabolic rates, especially in residential settings where occupants engage in activities other than sedentary ones. Thus, we have decided to extent the predictive capabilities of Gagge's two-node model by substituting its simple linear, temperature-based active system model with Fiala's non-linear, temperature-based active system model, which has been reviewed in Section 2.3.

### 4.2. Fiala's DTS model

Once having determined the static comfort part, Fiala derived the dynamic component of human thermal sensation by linear regression using the following rearranged equation:

$$\boldsymbol{Y} = \left[\boldsymbol{tanh}^{-1}\left(\frac{\boldsymbol{DTS}}{\boldsymbol{3}}\right) - \boldsymbol{a} \cdot \boldsymbol{\Delta T_{sk,mean}} - \boldsymbol{g}\right] \cdot (\boldsymbol{1} + \boldsymbol{g}) = \boldsymbol{b} \cdot \frac{\boldsymbol{\partial T_{sk,mean}}}{\boldsymbol{\partial t}} \quad 8$$

The linear regression was run using a limited set of experimental data coming from only two exposures to sudden step-changes in air temperature: 28-18-28°C and 28-48-28°C [29]. Additional experimental data from cyclical temperature variations were then used to validate the model for transient conditions. In Figure 4, observed thermal sensation votes (TSV) are compared with Fiala's predicted DTS values for two exposures to cyclical temperature fluctuations [35]. Fiala's predictions (in cyan in Figure 4) use the updated Gagge's 2-node model coupled with Fiala's DTS model. The predicted DTS values agree reasonably well for the slower sinusoidal changes of air temperature ($\frac{\partial T_a}{\partial t} = 5\ K/h$ for Condition I-2 in Figure 4) but the model is not able to follow faster fluctuations of air temperature ($\frac{\partial T_a}{\partial t} = 10.9\ K/h$ for Condition I-1 in Figure 4). Given these limitations, we have decided to update Fiala's $b$ coefficient by using additional experimental data coming from both the cyclical conditions of Dataset II [36] and the step-change conditions of Dataset III

[37,38], which have been illustrated in Section 3.1. The linear regression procedure to obtain $b$ is the same as the one used by Fiala but the body core and skin temperatures are simulated using the updated Gagge's 2-node model described in Section 4.1.

By looking at the relationship between $Y$ and $\frac{\partial T_{sk,mean}}{\partial t}$ in Figure 1 we can see that the dynamic component of thermal sensation strongly depends on the rate of change of the skin temperature, however it does not grow indefinitely for high values of $\frac{\partial T_{sk,mean}}{\partial t}$; but rather reaches a positive and negative asymptote. Thus, we model this asymptotic behaviour using the classical hyperbolic tangent and, thus, we apply regression analysis to the linearized equation $Y = b \cdot tanh\left(\frac{\partial T_{sk,mean}}{\partial t}\right)$ instead of the form $Y = b \cdot \frac{\partial T_{sk,mean}}{\partial t}$ used in Equation 8. The resulting linear model for cooling gradients has a coefficient of determination $\mathrm{R}^2$ equal to $0.728$, hence our predictor $tanh\left(\frac{\partial T_{sk,mean}}{\partial t}\right)$ explains about 73% of the variability of our dependent variable Y. The $F - ratio$ is equal to $369.5$ and the p-value associated with the model as a whole is very small, $p < 7.56e^{-41}$, which means that the regression model is a good fit of the data. The resulting linear model for warming gradients has a coefficient of determination $\mathrm{R}^2$ equal to $0.552$, an $F - ratio$ equal to $167.3$ and a small p-value associated with the model as a whole, $p < 1.90e^{-25}$. We have checked that the key assumptions of linear regression (normality, homoscedasticity and no autocorrelation of the residual errors) are met. The resulting updated DTS model has the form:

$$\boldsymbol{DTS = 3 \cdot tanh\left[a \cdot \Delta T_{sk,mean} + g + \left[b \cdot tanh\left(\frac{\partial T_{sk,mean}}{\partial t}\right)\right] \cdot \frac{1}{(1+g)}\right]} \quad (9)$$

where the coefficient b is equal to $0.3412$ for cooling gradients $\frac{\partial T_{sk,mean}}{\partial t}^{(-)}$ and $0.2755$ for warming gradients $\frac{\partial T_{sk,mean}}{\partial t}^{(+)}$.

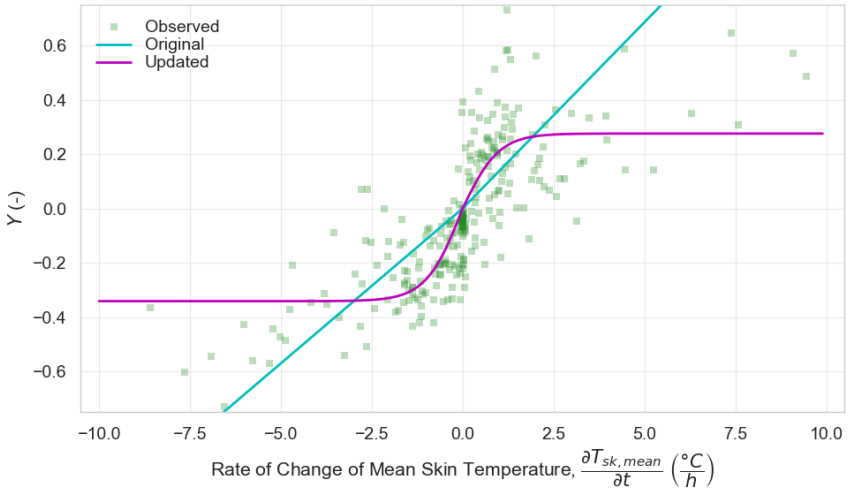


Figure 1. The term Y as a function of $\frac{\partial T_{sk,mean}}{\partial t}$. Observed data are from Dataset II [36] and Dataset III [37,38].

### 4.3. DPD model

Fanger's well-known non-linear relationship between $PMV$ and $PPD$ is derived from steady-state laboratory experiments involving 1300 subjects and is given by:

$$\boldsymbol{PPD = 1 - 0.95 \cdot e^{(-0.03353 \cdot PMV^4 - 0.2179 \cdot PMV^2)}} \quad (10)$$

We derive a new dynamic version of Fanger's static PPD index by using the new Equations **Erreur ! Source du renvoi introuvable.**. The reason behind this modelling approach is twofold: the parameter $a$ accounts for the fact that the dynamic thermal perception horizontally shifts subjects' neutral conditions (at which maximum comfort is felt) towards warm thermal sensations during warming transients and cold thermal sensations during cooling transients. This is due to the warming and cooling overshoots perceived during warming and cooling transients respectively. At the same time, a vertical thermal comfort shift expressed by the parameter $b$ accounts for the alliesthesial effect: in warm conditions cooling transients elicit pleasure and, thus, increased satisfaction, while warming transients elicit displeasure and, thus, decreased satisfaction. The opposite is true for cold conditions. For the literature on the phenomenon of thermal alliesthesia the reader is referred to the works of Cabanac [43], Attia [44], Zhang [25–27], Parkinson [45] and Vellei & Le Dréau [46].

The data used to derive the new dynamic $PPD$ relation comes from the warm conditions of Dataset II since too few data of Dataset II is related to cold conditions [36]. In Dataset II, the observed percentage of dissatisfied subjects, *observed* $PD$, is interpreted from a binary thermal acceptability scale and is defined as the ratio of thermal unacceptability votes to total votes. Fanger's PPD index is derived using a different definition for the percentage of dissatisfied subjects, which is the percentage of people voting above warm or below cool (≥2 or ≤-2) on the 7-point ASHRAE thermal sensation scale. This method of derivation of $PPD$ is suitable under steady-state conditions. However, under dynamic conditions, warm and cold thermal sensations can be associated with satisfaction/pleasure if positive alliesthesia is elicited, hence Fanger's derivation of the $PPD$ index is suitable to predict thermal comfort only under steady-state conditions.

To obtain the unknown parameters $a$ and $b$ of Equation 11 we use the Nelder-Mead Algorithm (as implemented in the python function *scipy.optimize.minimize*) to minimize the $RMSE$ for both cooling and warming transients under warm conditions. The resulting $a$ and $b$ parameters for cooling gradients are equal to $-0.2151$ and $-0.0251$, while for the warming gradients are equal to $-0.5424$ and $-0.0679$. These coefficients are valid for warm exposures since they are both derived from the warm conditions of Dataset II. In cold conditions, it is assumed that cooling and warming overshoots have the same magnitude than in warm conditions. Thus, the coefficient $a$ is the same as derived above. Based on the alliesthesial effect which states that warming gradients are pleasurable in cold conditions but unpleasant in warm conditions and, on the contrary, cooling gradients are pleasurable in warm conditions but unpleasant in cold conditions, it is assumed that the coefficient $b$ for cold conditions has the opposite sign than the coefficient derived above for warm conditions.

$$\boldsymbol{DPD = 1 - 0.95 \cdot e^{\left(-0.03353 \cdot \left(TSV + a \cdot tanh\left[\frac{\partial T_{sk,mean}}{\partial t}\right]\right)^4 - 0.2179 \cdot \left(TSV + a \cdot tanh\left[\frac{\partial T_{sk,mean}}{\partial t}\right]\right)^2\right) + b \cdot tanh\left[\frac{\partial T_{sk,mean}}{\partial t}\right]}} \qquad 11$$

where:

- in warm and cold conditions, the coefficient $a$ is equal to $-0.2151$ for cooling gradients $\frac{\partial T_{sk,mean}}{\partial t}^{(-)}$ and $-0.5424$ for warming gradients $\frac{\partial T_{sk,mean}}{\partial t}^{(+)}$,
- in warm conditions, the coefficient b is equal to $-0.0251$ for cooling gradients $\frac{\partial T_{sk,mean}}{\partial t}^{(-)}$ and $-0.0679$ for warming gradients $\frac{\partial T_{sk,mean}}{\partial t}^{(+)}$, while in cold conditions

the opposite is true, the coefficient b is equal to $+0.0251$ for cooling gradients $\frac{\partial T_{sk,mean}}{\partial t}^{(-)}$ and $+0.0679$ for warming gradients $\frac{\partial T_{sk,mean}}{\partial t}^{(+)}$.

The novel DPD model is plotted in Figure 2 for warm conditions (left) and cold conditions (right).

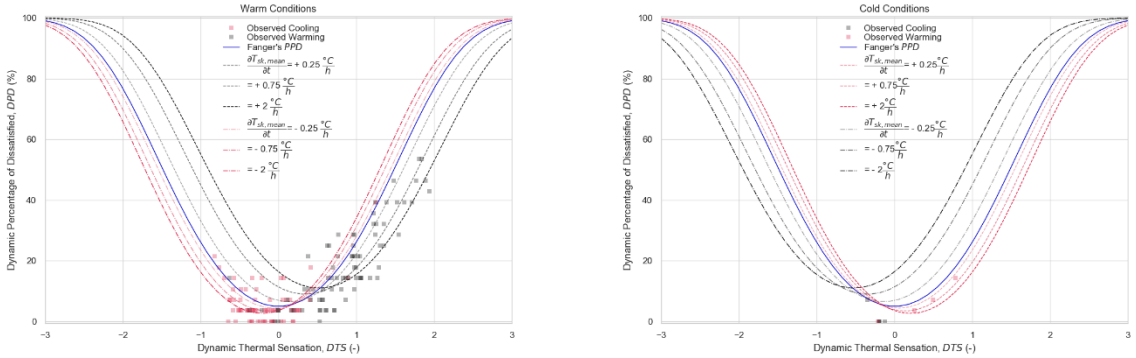


Figure 2. Updated Fanger's PPD relation for warm conditions (left) and cold conditions (right). The observed data comes from Dataset II [36].

## 5. Results

### 5.1. Skin and body core temperatures

In this Section, we show the performances in terms of RMSE of the updated Gagge's two-node model against the original ones for predicting body core and mean skin temperatures. From Figure 3 we can see the significant contribution of Fiala's active system in improving the prediction of the body core temperatures. However, there is not such improvement for the mean skin temperatures, except for the very cold exposure of condition 0-4.

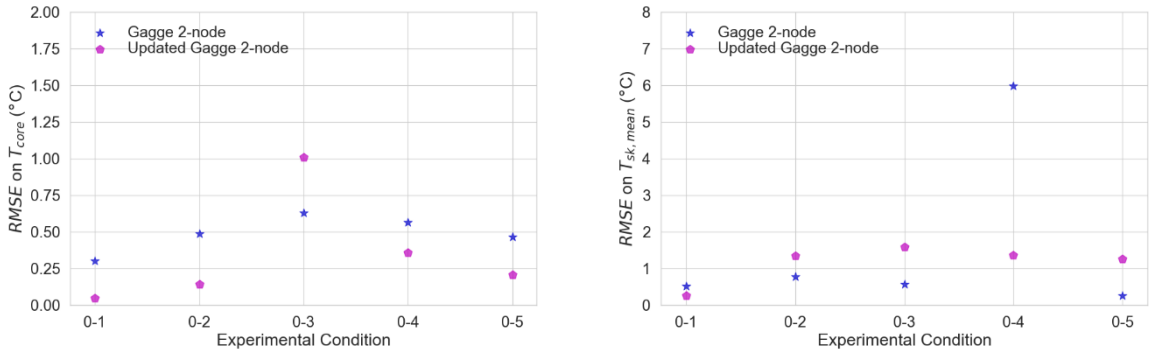


Figure 3. RMSE of the updated Gagge's two-node model against the original one for the different experimental conditions of Dataset 0.

### 5.2. Thermal sensation votes

In this Section, we show the performances in terms of RMSE of the updated Fiala's DTS model against the original one. Fanger's PMV model is also included for comparison.

Sedentary activity level

From Figure 6 we can see that for the cyclical temperature variations of Dataset I and II and the step-change conditions of Dataset III, the updated Fiala's DTS plus the Gagge's two-node model give the best results, generally performing better than Fanger's PMV model, with the difference more accentuated for the more dynamic conditions.

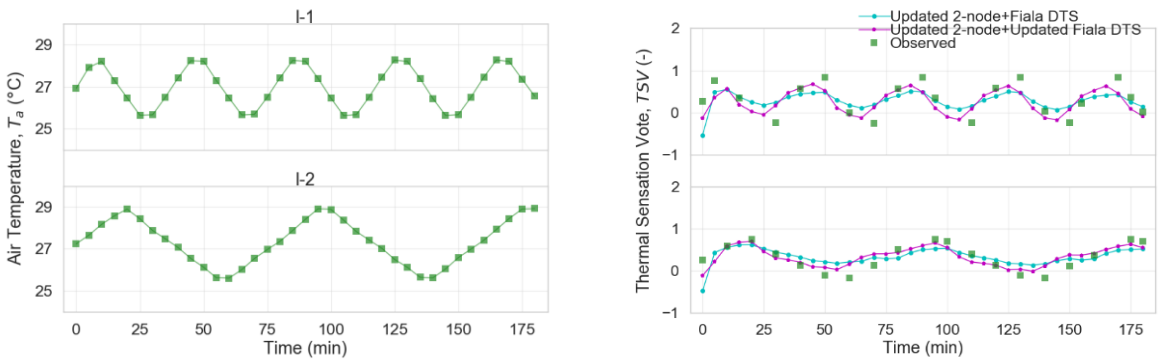


Figure 4. Air temperature ($T_a$, left) and thermal sensation ($TSV$, right) for the 2 cyclical temperature variations (Conditions 1 and 2) of Dataset I [35]. Observed data are shown in green.

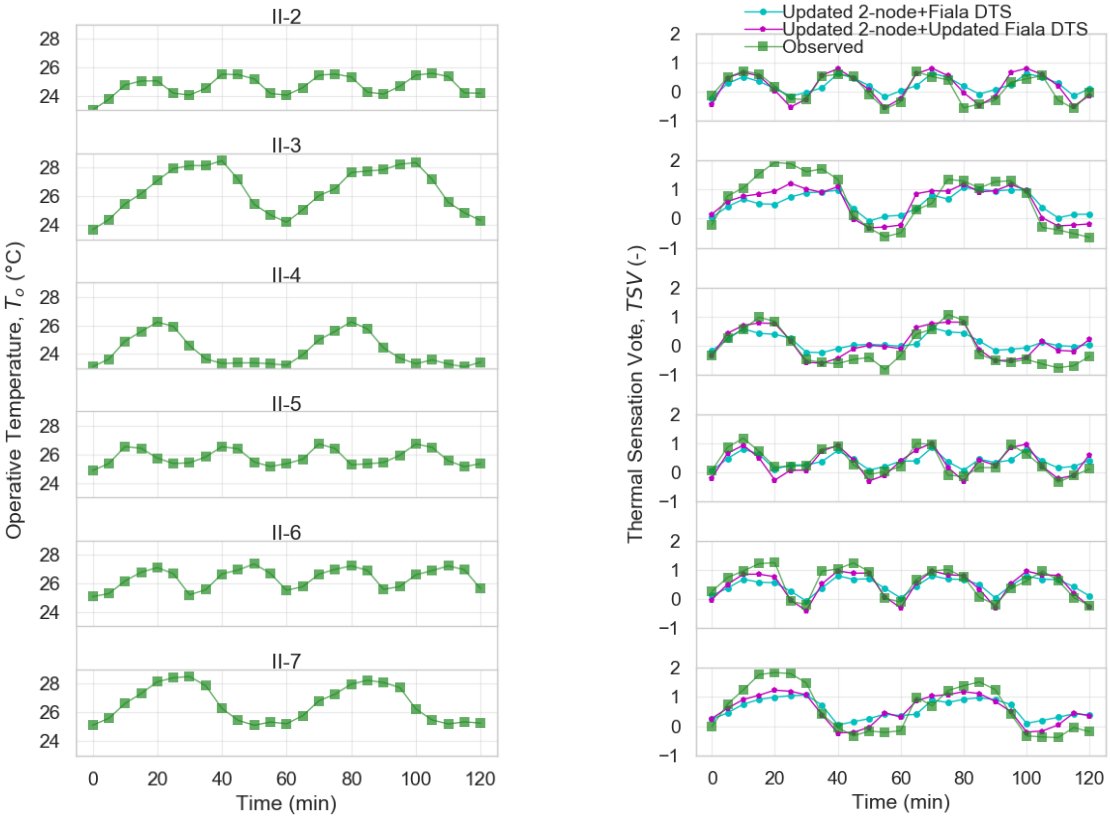


Figure 5. Operative temperature ($T_o$, left) and thermal sensation ($TSV$, right) for the 6 cyclical temperature variations (Conditions 2-7) of Dataset II [36]. Observed data are shown in green.

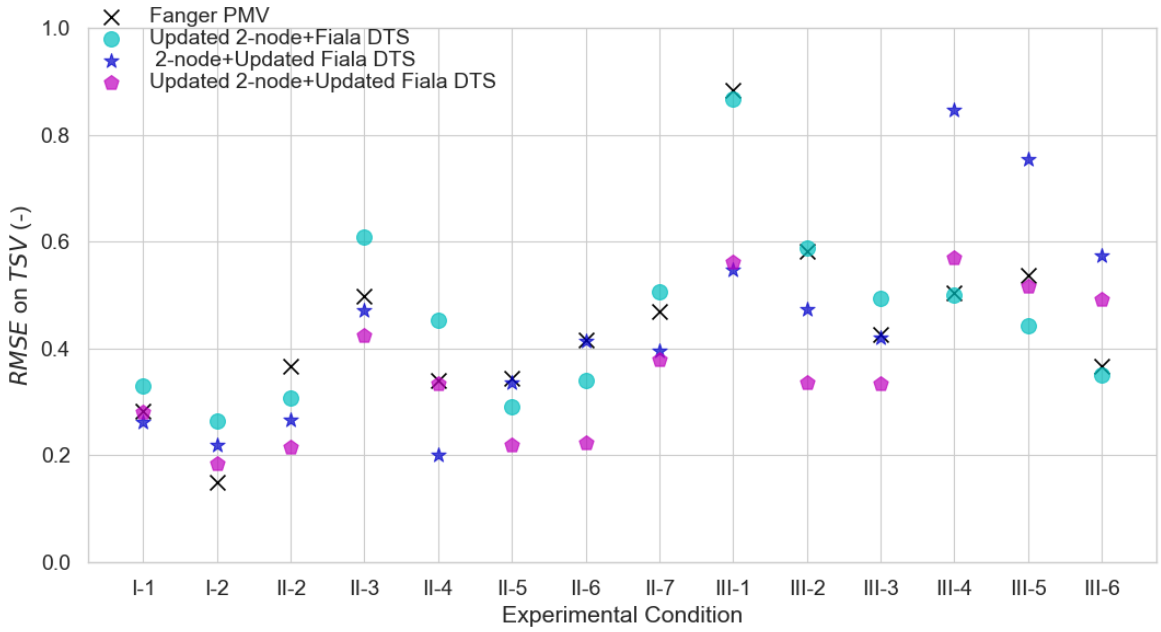


Figure 6. RMSE on TSV of the different tested models for the different experimental conditions of Dataset I (cyclical conditions), II (cyclical conditions) and III (step-change conditions).

Transient work

From Figure 7 we can see that the updated Gagge's two-node model gives better results than the original one in the majority of the studied conditions, showing how determinant is the role of the Fiala's active system for conditions of transient work. Gagge's two-node model also performs better than Fanger's PMV model. We can further see that the predictions of Fiala's updated DTS model are similar than those of the original one. In fact, during transient work the dynamic thermal sensation is dominated by the body core temperature rather than by the mean skin temperature. Finally, by comparing Figure 6 and Figure 7, we can observe that the performances during transient work are generally worse than during sedentary conditions.

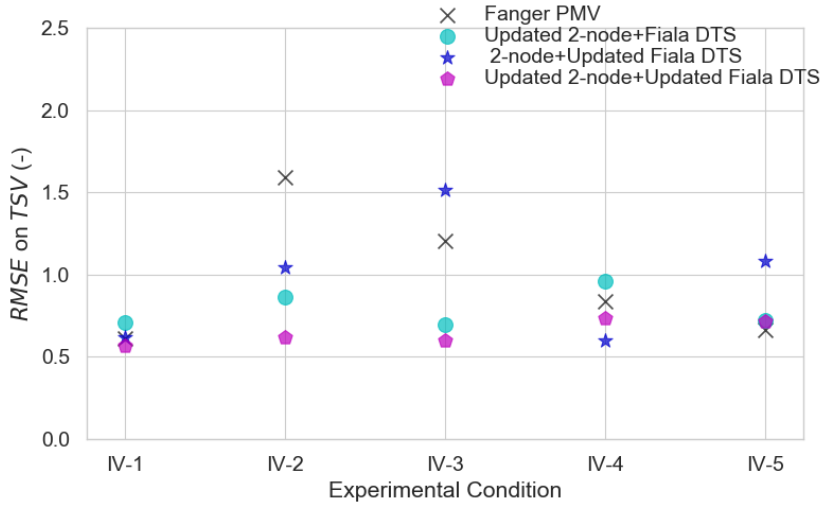


Figure 7. RMSE on TSV of the different tested models for the different experimental conditions of Dataset IV.

### 5.3. Percentage of Dissatisfied Occupants

In this Section, we show the performances in terms of RMSE of the updated Fanger's PPD (named DPD) against the original one. From Figure 8 we can see that the updated model is particularly important for improving the prediction during the most dynamic cyclical conditions II-3 and II-7 of Database II.

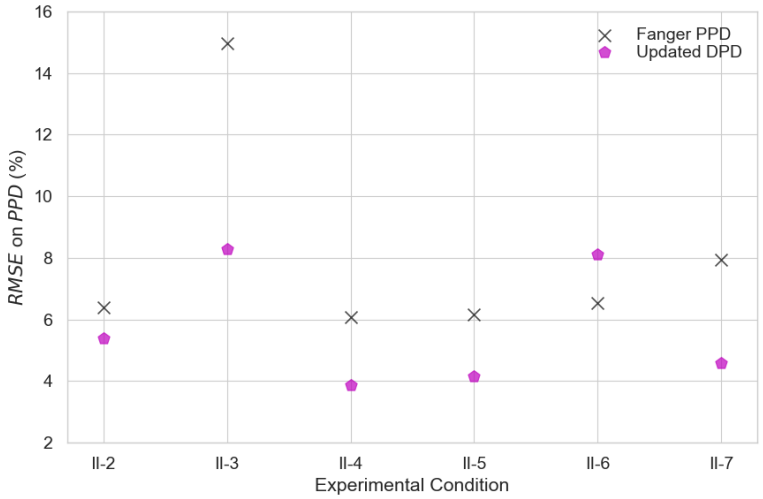


Figure 8. RMSE on PPD of the different tested models for the different experimental conditions of Dataset II.

## 6. Conclusions

In this paper, we describe, evaluate and provide a new simple tool for predicting dynamic thermal comfort under uniform conditions. This tool is based on previous well-known and esteemed works: Gagge's 2-node model, Fiala's DTS model and Fanger's PPD model, which we have updated using recent knowledge and new empirical data. Gagge's 2-node model has been updated using Fiala's empirical control equations for sweating, shivering, and cutaneous vasomotion. The dynamic component of Fiala's DTS model has been updated using new data from both cyclical and step-change thermal conditions. Finally, we have used a new framework and new data from cyclical thermal conditions to update the form of the traditional Fanger's PPD model into a new dynamic index. We show that our updated models have better performances than the original ones and also outperform Fanger's model, especially for very dynamic conditions far from the neutrality. The simplicity and low computational cost of the proposed tool are important advantages over more-complex and more computationally expensive multi-segment and multi-node thermo-physiological models.


### Acknowledgements

This research was funded by the French National Research Agency, project ANR CLEF (ANR-17-CE22-0005-01). We thank Edouard Walther for providing us with the initial Python version of Gagge's two-node model.


### Supplementary materials

The models coded in Python are available to download at https://gitlab.univ-lr.fr/jledreau/dynamic-thermal-comfort.

## 7. References


[1] K. Katić, R. Li, W. Zeiler, Thermophysiological models and their applications: A review, Build. Environ. 106 (2016) 286–300. doi:10.1016/j.buildenv.2016.06.031.

[2] B. Koelblen, A. Psikuta, A. Bogdan, S. Annaheim, R.M. Rossi, Thermal sensation models: Validation and sensitivity towards thermo-physiological parameters, Build. Environ. 130 (2018) 200–211. doi:10.1016/j.buildenv.2017.12.020.

[3] S. Tanabe, K. Kobayashi, J. Nakano, Y. Ozeki, M. Konishi, Evaluation of thermal comfort using combined multi-node thermoregulation (65MN) and radiation models and computational fluid dynamics (CFD), Energy Build. 34 (2002) 637–646. doi:10.1016/S0378-7788(02)00014-2.

[4] D. Fiala, K.J. Lomas, M. Stohrer, Computer prediction of human thermoregulatory and temperature responses to a wide range of environmental conditions, Int. J. Biometeorol. 45 (2001) 143–159. doi:10.1007/s004840100099.

[5] D. Fiala, G. Havenith, P. Bröde, B. Kampmann, G. Jendritzky, UTCI-Fiala multi-node model of human heat transfer and temperature regulation, Int. J. Biometeorol. 56 (2012) 429–441. doi:10.1007/s00484-011-0424-7.

[6] C. Huizenga, Z. Hui, E. Arens, A model of human physiology and comfort for assessing complex thermal environments, Build. Environ. 36 (2001) 691–699. doi:10.1016/S0360-1323(00)00061-5.

[7] B.R.M. Kingma, L. Schellen, A.J.H. Frijns, W.D. van Marken Lichtenbelt, Thermal sensation: a mathematical model based on neurophysiology, Indoor Air. 22 (2012) 253–262. doi:10.1111/j.1600-0668.2011.00758.x.

[8] D. Da Silva, Analyse de la flexibilité des usages électriques résidentiels : application aux usages thermiques, École Nationale Supérieure des Mines de Paris, 2011.

[9] M.-A. Leduc, A. Daoud, C. Le Bel, Developing winter residential demand response strategies for electric space heating, in: BS2011 12th Conf. Int. Build. Perform. Simul. Assoc., Sydney (AU), 2011.

[10] P. Morales-Valdés, A. Flores-Tlacuahuac, V.M. Zavala, Analyzing the effects of comfort relaxation on energy demand flexibility of buildings: A multiobjective optimization approach, Energy Build. 85 (2014) 416–426. doi:10.1016/j.enbuild.2014.09.040.

[11] J. Le Dréau, P. Heiselberg, Energy flexibility of residential buildings using short term heat storage in the thermal mass, Energy. 111 (2016) 991–1002. doi:10.1016/j.energy.2016.05.076.

[12] G. Masy, E. Georges, C. Verhelst, V. Lemort, P. André, Smart grid energy flexible buildings through the use of heat pumps and building thermal mass as energy storage in the Belgian context, Sci. Technol. Built Environ. 21 (2015) 800–811. doi:10.1080/23744731.2015.1035590.

[13] T.Q. Péan, J. Ortiz, J. Salom, Impact of Demand-Side Management on Thermal Comfort and Energy Costs in a Residential nZEB, Buildings. 7 (2017).

[14] T. Weiß, A.M. Fulterer, A. Knotzer, Energy flexibility of domestic thermal loads – a building typology approach of the residential building stock in Austria, Adv. Build. Energy Res. (2017) 1–16. doi:10.1080/17512549.2017.1420606.

[15] S. Agapoff, M. Jandon, T. Guiot, Impact of a tariff based heating load control on energy, comfort and environment : a parametric study in residential and office buildings, in: Int. SEEDS Conf. 2017 Sustain. Ecol. Eng. Des. Soc., Leeds (UK), 2017.

[16] P.O. Fanger, Thermal comfort: analysis and applications in environmental engineering, McGraw-Hill, 1972.

[17] A.P. Gagge, J.A.J. Stolwijk, Y. Nishi, Effective temperature scale based on a simple model of human physiological regulatory response, ASHRAE Trans. 77 (1971) 247–263.
[18] D. Fiala, K.J. Lomas, M. Stohrer, First principles modeling of thermal sensation responses in steady-state and transient conditions, in: ASHRAE Trans., 2003: pp. 179–186. doi:10.1590/S1517-838220080002000021.
[19] A.P. Gagge, A.P. Fobelets, L.G. Berglund, A standard predictive index of human response to the thermal environment., ASHRAE Trans. 92 (1986) 709–731.
[20] M. Fountain, C. Huizenga, A thermal sensation model for use by the engineering profession, 1995.
[21] T. Doherty, E. Arens, Evaluation of the physiological bases of thermal comfort models, ASHRAE Trans. 94 (1988) 1371–1385.
[22] L.G. Berglund, Mathematical models for predicting the thermal comfort response of building occupants, ASHRAE Trans. 84 (1978) 735–749.
[23] R.A. Haslam, An evaluation of models of human response to hot and cold environments, Loughborough University, UK, 1989.
[24] C. Smith, A Transient, Three-Dimensional Model of the Human Thermal System, Kansas State University, USA, 1991.
[25] H. Zhang, E. Arens, C. Huizenga, T. Han, Thermal sensation and comfort models for non-uniform and transient environments, part II: Local comfort of individual body parts, Build. Environ. 45 (2010) 389–398. doi:10.1016/j.buildenv.2009.06.015.
[26] H. Zhang, E. Arens, C. Huizenga, T. Han, Thermal sensation and comfort models for non-uniform and transient environments, part III: Whole-body sensation and comfort, Build. Environ. 45 (2010) 399–410. doi:10.1016/j.buildenv.2009.06.020.
[27] H. Zhang, E. Arens, C. Huizenga, T. Han, Thermal sensation and comfort models for non-uniform and transient environments: Part I: Local sensation of individual body parts, Build. Environ. 45 (2010) 380–388. doi:10.1016/j.buildenv.2009.06.018.
[28] S. Takada, S. Matsumoto, T. Matsushita, Prediction of whole-body thermal sensation in the non-steady state based on skin temperature, Build. Environ. 68 (2013) 123–133. doi:10.1016/j.buildenv.2013.06.004.
[29] A.P. Gagge, J.A.J. Stolwijk, J.D. Hardy, Comfort and thermal sensations and associated physiological responses at various ambient temperatures, Environ. Res. 1 (1967) 1–20. doi:https://doi.org/10.1016/0013-9351(67)90002-3.
[30] J.D. Hardy, J.A. Stolwijk, Partitional calorimetric studies of man during exposures to thermal transients, J. Appl. Physiol. 21 (1966) 1799–1806. doi:10.1152/jappl.1966.21.6.1799.
[31] J. Werner, M. Heising, W. Rautenberg, K. Leimann, Dynamics and topography of human temperature regulation in response to thermal and work load, Eur. J. Appl. Physiol. Occup. Physiol. 53 (1985) 353–358. doi:10.1007/BF00422853.
[32] C.A. Walsh, T.E. Graham, Male-female responses in various body temperatures during and following exercise io cold air, Aviat. Sp. Environ. Med. 57 (1986) 966–973.
[33] P. Chappuis, P. Pittet, E. Jequier, Heat storage regulation in exercise during thermal transients, J. Appl. Physiol. 40 (1976) 384–392. doi:10.1152/jappl.1976.40.3.384.
[34] J.A. Stolwijk, J.D. Hardy, Partitional calorimetric studies of responses of man to thermal transients., J. Appl. Physiol. 21 (1966) 967–977. doi:10.1152/jappl.1966.21.3.967.
[35] C.H. Sprague, P.E. McNall Jr, The effects of fluctuating temperature and relative

humidity on the thermal sensation (thermal comfort) of sedentary subjects, ASHRAE Trans. 76 (1970) 146–156.
[36] F. Zhang, R. de Dear, C. Candido, Thermal comfort during temperature cycles induced by direct load control strategies of peak electricity demand management, Build. Environ. 103 (2016) 9–20. doi:10.1016/j.buildenv.2016.03.020.
[37] X. Du, B. Li, H. Liu, D. Yang, W. Yu, J. Liao, Z. Huang, K. Xia, The Response of Human Thermal Sensation and Its Prediction to Temperature Step-Change (Cool-Neutral-Cool), PLoS One. 9 (2014) e104320. doi:10.1371/journal.pone.0104320.
[38] H. Liu, J. Liao, D. Yang, X. Du, P. Hu, Y. Yang, B. Li, The response of human thermal perception and skin temperature to step-change transient thermal environments, Build. Environ. 73 (2013) 232–238. doi:10.1016/j.buildenv.2013.12.007.
[39] R.G. Nevins, R.R. Gonzalez, Y. Nishi, A.P. Gagge, Effect of changes in ambient temperature and level of humidity on comfort and thermal sensations, ASHRAE Trans. 81 (1975) 169–182.
[40] R. Nielsen, B. Nielsen, Influence of skin temperature distribution on thermal sensation in a cool environment, Eur. J. Appl. Physiol. Occup. Physiol. 53 (1984) 225–230. doi:10.1007/BF00776594.
[41] M.. Fahnestock, F.E. Boys, F. Sargent, L.D. Siler, Energy Cost, Comfort, and Physiological Responses to Physical Work in 95F-50% rh and 75%-45% rh Environments, ASHRAE Trans. 73 (1967) 1–20.
[42] D. Tan, H. Liu, Y. Wu, The Response of Human Thermal Perception and Skin Temperature to Step-Changed Activity Level, Int. J. Environ. Sci. Dev. 8 (2017) 425–429. doi:10.18178/ijesd.2017.8.6.991.
[43] M. Cabanac, Sensory Pleasure, Q. Rev. Biol. 54 (1979) 1–29. doi:10.1086/410981.
[44] M. Attia, Thermal pleasantness and temperature regulation in man, Neurosci. Biobehav. Rev. 8 (1984) 335–342. doi:10.1016/0149-7634(84)90056-3.
[45] T. Parkinson, R. De Dear, C. Candido, Thermal pleasure in built environments: Alliesthesia in different thermoregulatory zones, Build. Res. Inf. 44 (2016) 20–33. doi:10.1080/09613218.2015.1059653.
[46] M. Vellei, J. Le Dréau, A novel model for evaluating dynamic thermal comfort under demand response events, Build. Environ. 160 (2019) 106–215. doi:10.1016/j.buildenv.2019.106215.